Journal of Power Sources 184 (2008) 437–443

Contents lists available at ScienceDirect

Journal of Power Sources

journal homepage: www.elsevier.com/locate/jpowsour

Novel electrospun poly(vinylidene fluoride-*co*-hexafluoropropylene)–in situ SiO_2 composite membrane-based polymer electrolyte for lithium batteries

Prasanth Raghavan[a], Jae-Won Choi[a], Jou-Hyeon Ahn[a,*], Gouri Cheruvally[a], Ghanshyam S. Chauhan[a], Hyo-Jun Ahn[b], Changwoon Nah[c]

[a] *Department of Chemical and Biological Engineering and Engineering Research Institute, Gyeongsang National University, 900 Gajwa-dong, Jinju 660-701, Republic of Korea*
[b] *School of Nano and Advanced Materials Engineering and Engineering Research Institute, Gyeongsang National University, 900 Gajwa-dong, Jinju 660-701, Republic of Korea*
[c] *Department of Polymer-Nano Science and Technology, Chonbuk National University, 664-14 Duckjin-dong, Jeonju 561-756, Republic of Korea*

ARTICLE INFO

Article history:
Received 28 December 2007
Received in revised form 22 February 2008
Accepted 17 March 2008
Available online 22 March 2008

Keywords:
Polymer electrolyte
Electrospinning
Lithium batteries
Fibrous membrane
In situ SiO_2

ABSTRACT

Composite membranes of poly(vinylidene fluoride-*co*-hexafluoropropylene) {P(VdF-HFP)} and different composition of silica have been prepared by electrospinning polymer solution containing in situ generated silica. These membranes are made up of fibers of 1–2 μm diameters. These fibers are stacked in layers to produce fully interconnected pores that results in high porosity. Polymer electrolytes were prepared by immobilizing 1 M $LiPF_6$ in ethylene carbonate (EC)/dimethyl carbonate (DMC) in the membranes. The composite membranes exhibit a high electrolyte uptake of 550–600%. The optimum electrochemical properties have been observed for the polymer electrolyte containing 6% in situ silica to show ionic conductivity of 8.06 mS cm^{-1} at 20 °C, electrolyte retention ratio of 0.85, anodic stability up to 4.6 V versus Li/Li^+, and a good compatibility with lithium metal resulting in low interfacial resistance. A first cycle specific capacity of 170 mAh g^{-1} was obtained when the polymer electrolyte was evaluated in a Li/lithium iron phosphate ($LiFePO_4$) cell at 0.1 C-rate at 25 °C, corresponding to 100% utilization of the cathode material. The properties of composite membrane prepared with in situ silica were observed to be comparatively better than the one prepared by direct addition of silica.

1. Introduction

Polymer electrolytes have attracted great interest compared to their liquid counterparts, which provide the advantages to develop lighter and safer batteries with longer shelf life, leak proof construction and easy fabrication into desired shape and size [1]. The researchers aim at developing polymer electrolytes with good ambient temperature conductivity and stable electrode/electrolyte interfacial properties with minimum resistance to ion transportation [2–4]. For preparing polymer electrolytes, poly(vinylidene fluoride) (PVdF) [5], poly(vinylidene fluoride-*co*-hexafluoropropylene) {P(VdF-HFP)} [6], poly(methyl methacrylate) [7] and polyacrylonitrile (PAN) [8] have been widely studied as host polymers. Ceramic fillers such as $BaTiO_3$, ZrO_2, Al_2O_3, TiO_2 and SiO_2 are also incorporated along with the host polymer to fabricate composite polymer electrolytes [9–12]. These fillers improve the ionic conductivity of the polymer electrolyte by reducing the crystallinity of the polymer and also introduce Lewis acid–base interactions between the polar surface groups of the inorganic filler and the electrolyte ionic species [10,11]. In addition, ceramic fillers enhance the mechanical properties of the polymer electrolytes and improve the cation transference number and interfacial stability between the electrolyte and lithium metal electrode [12].

The membrane properties such as porosity and uniformity of pore distribution are dependent on its processing method. Different methods such as solvent casting [13], plasticizer extraction [14,15], phase inversion [16–19] and electrospinning [5,6,20–25] have been reported for the membrane preparation. Electrospinning is an easy and versatile method which is gaining importance in recent years as membranes prepared by employing this method have controlled properties. The electrospun polymer membranes consist of thin fibers of micron/sub-micron diameters with high specific surface area. The interlaying of fibers generates large porosity with fully interconnected pore structure that facilitates easy transport of ions, and serves as good host matrices for polymer electrolytes. From the electrochemical characterization studies of polymer electrolytes based on the electrospun membranes of PVdF [5,20–23], P(VdF-HFP) [6,24] and PAN [25], their potential for application in lithium batteries has been demonstrated.

The properties of composite polymer electrolytes, especially ionic conductivity, are influenced by the type and size of the ceramic particle incorporated. The smaller particles provide more

* Corresponding author. Tel.: +82 55 751 5388; fax: +82 55 753 1806.
E-mail address: jhahn@gsnu.ac.kr (J.-H. Ahn).

0378-7753/$ – see front matter © 2008 Elsevier B.V. All rights reserved.
doi:10.1016/j.jpowsour.2008.03.027

pronounced effects. Because of the high surface area of the nano-sized ceramic particles, their incorporation into the polymer host by mechanical blending leads to the minimization of the advantages by their aggregation. Incorporation of silica filler into the polymer matrix by its in situ generation would be more advantageous compared to the mechanical blending in providing a uniform distribution of the non-aggregated particles [26,27]. He et al. reported good performance for the composite polymer electrolyte based on P(VdF-HFP) membrane produced by phase inversion method, incorporating in situ generated silica [26]. In the present study, we report for the first time the properties of the novel composite polymer membrane based on P(VdF-HFP)–SiO_2 prepared by electrospinning polymer solution containing in situ generated silica. The electrochemical properties of the polymer electrolytes based on these membranes have been studied to evaluate their suitability for use in lithium batteries.

2. Experimental

P(VdF-HFP) (Kynar Flex 2801, $M_w = 4.77 \times 10^5$, VdF/HFP ratio: 88/12, Elf Atochem) was vacuum dried at 60 °C for 24 h before use. Acetone and *N*,*N*-dimethylacetamide (DMAc) (HPLC grades), lithium hexafluorophosphate ($LiPF_6$), ethylene carbonate (EC), dimethyl carbonate (DMC), tetraethoxy silane (TEOS) (Aldrich) and ammonium hydroxide (28% NH_3 in water, Daejung Chem.) were used as received. Fumed silica (particle size: 3–12 nm, surface area: 200 $m^2\,g^{-1}$) was vacuum dried for 24 h at 90 °C before use.

Three types of P(VdF-HFP) fibrous membranes (a) without silica, (b) with 3, 6 and 9% of in situ generated silica and (c) with 6% directly added silica were prepared by electrospinning the following solutions, respectively.

(a) A 16% solution of P(VdF-HFP) in acetone/DMAc (7:3, w/w) was prepared by magnetic stirring for 4 h at room temperature.
(b) A 14% solution of P(VdF-HFP) in acetone/DMAc (7:3, w/w) was first prepared by magnetic stirring for 4 h at room temperature. For generating in situ silica, a small quantity of ammonium hydroxide (3–4 drops) was added to the polymer solution, which was followed by dropwise addition of the required quantity of TEOS under vigorous stirring. The stirring was continued for 4 h at room temperature to generate silica according to the following equation [27]:

$$Si(OC_2H_5)_4 + 4H_2O \rightarrow Si(OH)_4 + 4C_2H_5OH \quad \text{(hydrolysis)}$$

$$Si(OH)_4 \rightarrow SiO_2 + 2H_2O \quad \text{(condensation)}$$

(c) A 14% solution of P(VdF-HFP) in acetone/DMAc (7:3, w/w) containing 6% silica was prepared by mechanical mixing in a ball mill for 1 h at room temperature in a Teflon container. The solution was degassed to remove the air bubbles before electrospinning.

All electrospinning experiments were performed at 25 °C following the typical procedure as described in detail in our earlier publication [6]. The essential electrospinning parameters were as follows: applied voltage 20 kV, distance between the tip of the spinneret and collector 16 cm, needle size 0.6 mm, solution feed rate 0.1 mL/min and collector drum rotation 140 rpm. Electrospun membranes of average thickness 150 μm were collected on a thin aluminum foil and were vacuum dried at 60 °C for 12 h before use.

Thermal properties of the electrospun membranes were evaluated by differential scanning calorimetry (DSC: 2010 TA Instruments) at a heating rate of 10 °C min^{-1} under an N_2 atmosphere from 50 to 200 °C and thermogravimetric analysis (TGA: SDT-Q600 TA Instruments) at a heating rate of 10 °C min^{-1} under N_2 atmosphere from 30 to 600 °C. The mechanical properties were evaluated according to ASTM D638. The porosity of the membrane was determined by the *n*-butanol uptake method [6]. The surface morphology was observed with scanning electron microscope (SEM: JEOL JSM 5600) and field emission-SEM (FE-SEM: Hitachi S-4800) and the average fiber diameter (AFD) was estimated from the micrographs taken at high magnification.

The electrolyte uptake by the membrane was studied by soaking the membrane in electrolyte for different time intervals [6]. The leakage properties of the soaked electrolytes were measured according to the procedure reported by Kim et al. [21]. The fibrous membrane was immersed in the electrolyte for 4 h to reach the equilibrium state. The residual electrolyte on the surface of the membrane was wiped off with filter paper. The membrane was then placed between two filter papers and squeezed by pressing with a standard weight kept above. The weight changes of the membrane were measured for every 15 min. The leakage of the electrolyte was calculated using the equation:

$$R = \frac{M_{PE}}{M_{PE,saturated}}$$

where R is the relative absorption ratio of the liquid electrolyte, $M_{PE,saturated}$ is the mass of the polymer electrolyte when the membrane is fully saturated with the liquid electrolyte, and M_{PE} is the mass of the polymer electrolyte after a time interval when the saturated polymer electrolyte is squeezed by pressing between two filter papers.

To measure the ionic conductivities of polymer electrolytes, membranes were soaked in the liquid electrolyte of 1 M $LiPF_6$ in EC/DMC (1:1, v/v) for 1 h and the conductivity was measured by the ac impedance analysis using stainless steel (SS) Swagelok® cells with 1M6 frequency analyzer over the temperature range 0–60 °C. The measurements were performed over the frequency range 10 mHz–2 MHz at an amplitude of 20 mV. The interfacial resistance R_f between the polymer electrolyte and lithium metal electrode was measured by the impedance response of Li/polymer electrolyte/Li cells over the frequency range 10 mHz–2 MHz at an amplitude of 20 mV. The electrochemical stability was determined by linear sweep voltammetry (LSV) of Li/polymer electrolyte/SS cells at a scan rate of 1 mV s^{-1} over the range of 2–5.5 V at 25 °C.

Two-electrode electrochemical coin cells were fabricated by placing the polymer electrolyte between lithium metal anode (300-μm thick, Cyprus Foote Mineral Co.) and carbon-coated lithium iron phosphate ($LiFePO_4$) cathode (23-μm thick). $LiFePO_4$ cathode-active material was synthesized in-house [28] and the cathode was prepared as its blend with conductive carbon and PVdF binder at a ratio of 80:10:10 by weight. Electrochemical tests of the Li/polymer electrolyte/$LiFePO_4$ cells were conducted between 2.5 and 4.0 V at a current density of 0.1 C using an automatic galvanostatic charge–discharge unit, WBCS3000 battery cycler (WonA Tech. Co.) at 25 °C. The activation of electrospun membrane to prepare the polymer electrolyte and the fabrication of test cells were carried out in an argon-filled glove box with a moisture level <10 ppm.

3. Results and discussion

Fig. 1 shows the SEM images of the membranes prepared by electrospinning of polymer solution without and with in situ generated silica. The ranges of fiber diameters obtained for the samples along with the AFDs are given in Table 1. The membrane without silica prepared by electrospinning a 16% solution has a uniform morphology with an AFD of 1.1 μm. Since the incorporation of silica results in an increase in viscosity and a subsequent deposition of

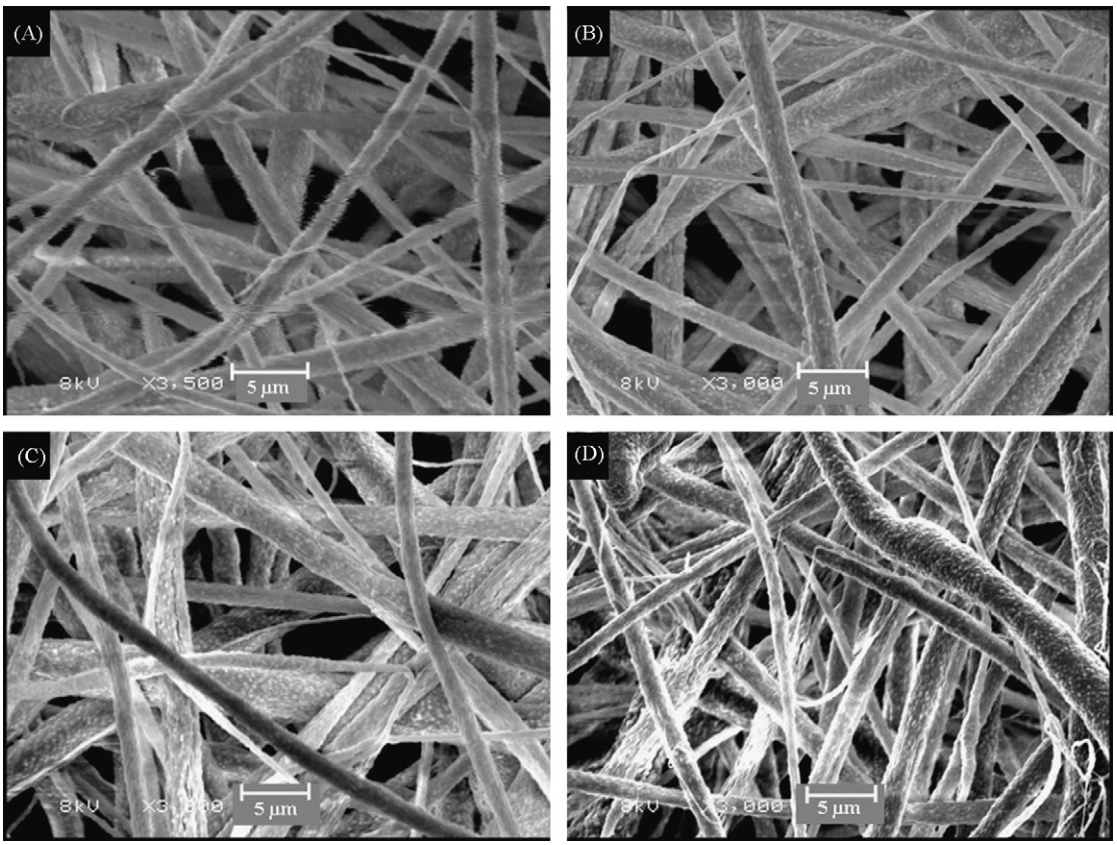

Fig. 1. SEM images of electrospun P(VdF-HFP) membranes with (A) 0% silica, (B) 3% in situ generated silica, (C) 6% in situ generated silica and (D) 9% in situ generated silica.

larger fibers, hence polymer solution with a lower concentration (14%) was utilized for preparing the composite membranes. This resulted in the membranes with relatively bead-free uniform morphology. It is observed that the in situ generated silica is uniformly distributed in the polymer matrix even at the higher content of 9%. The AFD of the composite membranes increases with increasing the silica content. Such an increase in AFD is attributed to the higher solution viscosity that leads to the ejection of larger drops from the needle which forms larger fibers on deposition [29]. Fig. 2 compares the FE-SEM images of the membranes containing 6% of in situ and directly added silica. Compared to the direct addition, in situ silica leads to a more uniform morphology of the membrane with a narrow fiber diameter range and a lower AFD. It is likely that the better distribution of the nano-sized in situ silica particles in the solution is achieved, and consequently a solution of lower viscosity is formed and fibers with smaller size are deposited.

The effect of incorporation of 6% in situ silica on the thermal properties of electrospun P(VdF-HFP) polymer is shown in Fig. 3. The polymer without filler has a melting transition at 159 °C (DSC analysis) with an estimated crystallinity of 74% based on a melting enthalpy of 104.7 J g^{-1} for the totally crystalline polymer [20,30]. The high crystallinity observed here (as the polymer in its powder form exhibits a crystallinity ~45% [20,30]) probably results from the orientation of the polymer when it is drawn to form nanofibers. By incorporating silica in the composition, melting point is slightly lowered though there is a considerable decrease of melting enthalpy, which corresponds to a crystallinity of ~50%. This observation confirms that the filler addition inhibits the crystallization process of the polymer. It increases the amorphous regions in the polymer, which is beneficial for the purpose of achieving a higher ionic conductivity. As seen in Fig. 3(B), the composite membrane has a slightly better thermal stability compared to the one without silica. The figure shows initial decomposition temperature of 450

Table 1
Properties of electrospun membranes and polymer electrolytes based on the membranes activated with 1 M $LiPF_6$ in EC/DMC

Properties	Silica content (wt%)				
	0	In situ			Direct
		3	6	9	6
Fiber diameter range (μm)	0.4–2.0	0.4–3.3	0.7–2.0	0.7–3.7	0.9–3.5
AFD (μm)	1.1	1.2	1.2	1.6	1.9
Porosity (%)	88	91	92	93	89
Electrolyte uptake (%)	425	556	592	620	491
Ionic conductivity at 20 °C (mS cm^{-1})	4.59	5.13	8.06	6.61	5.72
Electrolyte retention ratio (R)	0.83	0.84	0.85	0.82	0.84
Tensile strength (MPa)	6.5	7.4	10.9	12.3	9.0
Modulus (MPa)	9.2	14.5	14.8	15.7	14.9
Elongation at break (%)	71	69	58	50	56

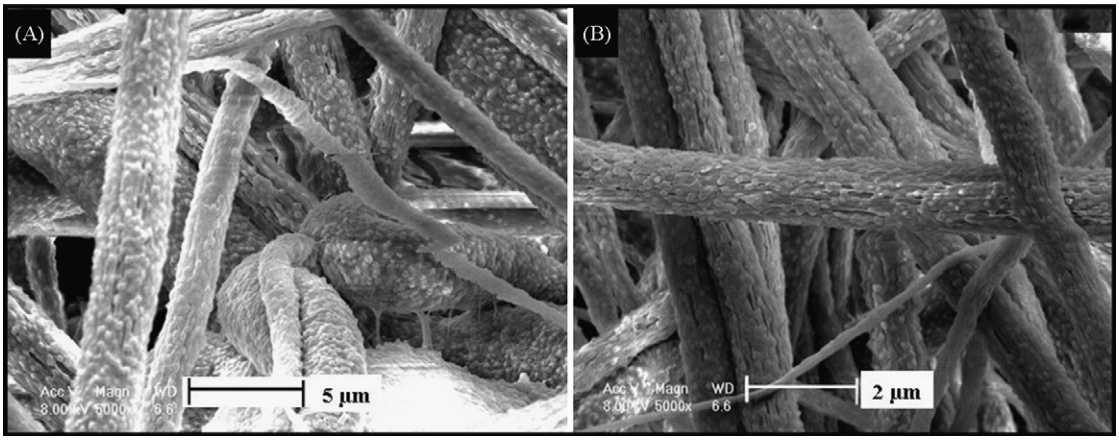

Fig. 2. FE-SEM images of electrospun P(VdF-HFP) membranes with 6% silica: (A) directly added silica and (B) in situ generated silica.

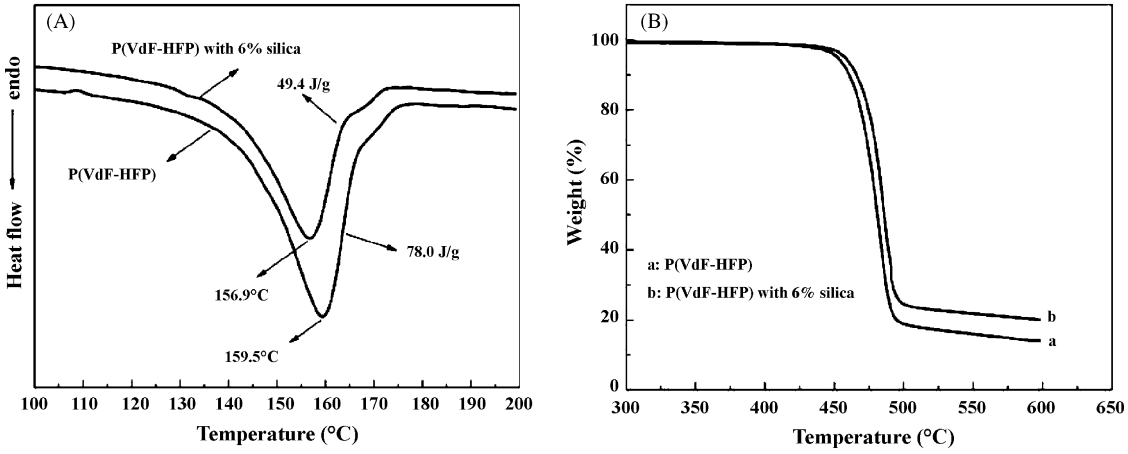

Fig. 3. Thermal properties of electrospun P(VdF-HFP) membranes with 0% silica and 6% in situ generated silica: (A) DSC and (B) TGA.

and 438 °C with a char yield nearly 20% versus 14%, respectively, at 600 °C. The difference in the char yield is equal to the amount of the in situ generated silica in the composite membrane.

Mechanical properties of the membranes are given in Table 1. Both ultimate tensile strength and Young's modulus show an increasing trend with silica content in the membrane, which is attributed to the reinforcing effect of the inorganic component incorporated in the polymer. The ceramic particles make the membrane slightly less flexible, and thus cause a decrease in % elongation at break. The membrane prepared with 6% of in situ generated silica and the one with 6% of directly added silica have nearly the comparable mechanical properties.

The interlaying of the fibers generates porous structure in the electrospun membrane. The results of porosity determination by *n*-butanol uptake method are given in Table 1. The porosity of the membranes varies in a narrow range of 88–93% showing a slight increase with the silica content. The narrow range of porosity results from the close similarities in the AFDs and the morphology of the membranes. Compared to the membrane porosities reported by Li et al. (59%, [6]) and Kim et al. (75%, [24]), values obtained in the present study are higher. This could arise from the differences in the processing parameters employed in the different studies. The higher porosity in the present study probably indicates a widely and more uniformly spaced fibrous structure compared to the earlier reports.

Polymer electrolytes were prepared by activating the membranes with the liquid electrolyte of 1 M $LiPF_6$ in EC/DMC. Fig. 4 presents a comparison of the electrolyte uptake of the membranes. The data was obtained by soaking the membranes in the liquid electrolyte for a period of 1 h. The electrolyte uptake is observed to increase steadily with the silica content. The maximum uptake value of each membrane is tabulated in Table 1. The absorption of the large quantities of liquid electrolyte by the composite membranes results from the high porosity of the membranes and the high amorphous content of the polymer. Thus, the electrolyte

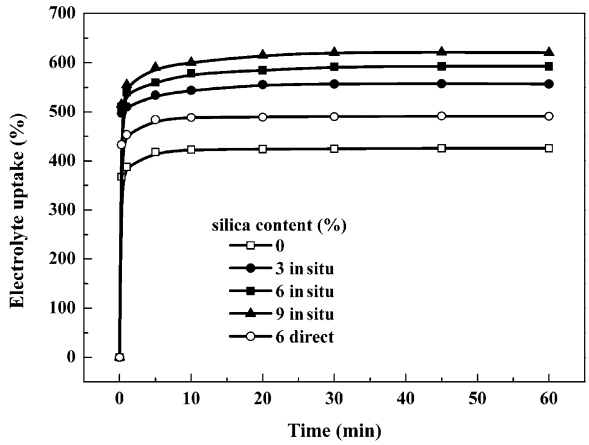

Fig. 4. Electrolyte uptake (%) of electrospun P(VdF-HFP) membranes with different silica contents (liquid electrolyte: 1 M $LiPF_6$ in EC/DMC).

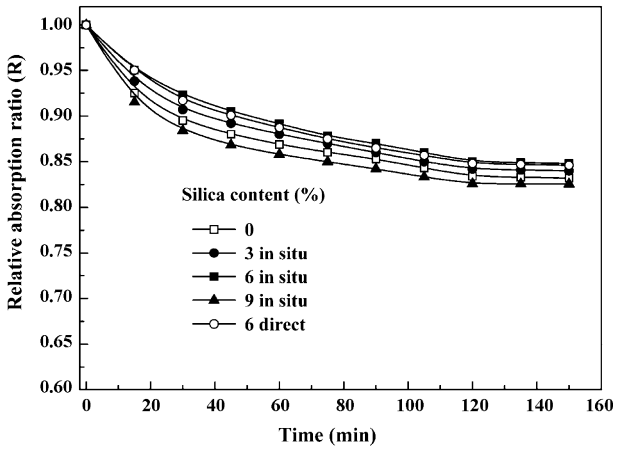

Fig. 5. Relative absorption ratio (R) of polymer electrolytes based on electrospun P(VdF-HFP) membranes with different silica contents.

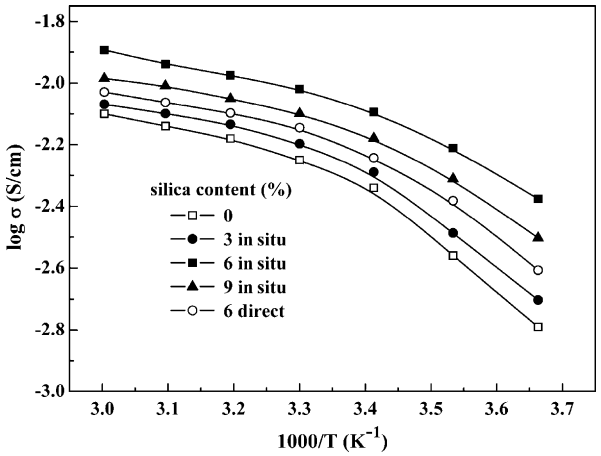

Fig. 6. Ionic conductivity at different temperatures of polymer electrolytes based on electrospun P(VdF-HFP) membranes with different silica contents.

uptake of ~600% achieved in this study is higher than that reported by Kim et al. [24] for a P(VdF-HFP) membrane of ~75% porosity. The fully interconnected pore structure makes fast penetration of the liquid into the membrane possible, and hence the uptake process is stabilized within the initial 15 min.

The high absorption of electrolyte by the porous membranes naturally leads to the speculation about the capability of the membranes to retain the absorbed electrolyte. Kim et al. have evaluated the leakage characteristics of electrospun P(VdF-HFP) membranes with 1 M $LiPF_6$ in EC/DMC/DEC (1:1:1, w/w/w) electrolyte solution over a period of 2 h [21]. They observed that the membranes with fibers of lower AFD are capable of retaining a larger proportion of the absorbed electrolyte with a minimum leakage. The relative absorption ratio R of the polymer electrolytes in this study is shown in Fig. 5. It is seen that the leakage characteristics tend to reach an equilibrium state within 2 h and all the polymer electrolytes exhibit a high retention of the electrolyte with a leakage <13, <16, and <18%, respectively, after 30 min, 1 h and 2 h. No leakage was observed after 2 h, as shown in Fig. 5. The electrolyte retention properties of the polymer electrolytes are comparable to those reported by Kim et al. for fibers with AFD ~1 μm [21]. It is believed that the high electrolyte retention by the polymer electrolytes originates from a combination of the high affinity of P(VdF-HFP) polymer for the electrolyte, the high surface area of the fibers, the reinforcing effect of the fillers in the membrane, and the unique pore structure of electrospun membrane.

The temperature dependence of the ionic conductivities of the polymer electrolytes in the range 0–60 °C is shown in Fig. 6. A smooth, linear enhancement in conductivity with increasing temperature was observed. The ionic conductivity values at 20 °C are compiled in Table 1. The incorporation of silica into the polymer matrix improves the conductivity with the maximum achieved for the sample with 6% of in situ silica. The enhancement in ionic conductivity of polymer electrolytes by the addition of ceramic fillers has also been reported in the earlier studies [10,11,26,27]. The primary reasons for the enhancement of conductivity have also been reported as the higher amorphous content of the polymer in the composite, the Lewis acid–base interactions between the filler particles and the electrolyte polar groups, and association between the filler particle and the polymer chains [10,11,27]. In the present case, enhancement of conductivity is also attributed to the same factors. The polymer electrolyte with 9% in situ silica shows lower ionic conductivity compared to the optimum, 6% in situ sample, although it exhibited a slightly higher electrolyte uptake. This indicates that the favorable properties imparted by silica towards ionic conductivity are masked at a higher content. Being insulating in nature, silica on its own impedes ionic conduction. The polymer electrolyte with 6% in situ silica shows ~1.4 times higher conductivity as compared to the polymer electrolyte with 6% directly added silica. This is a consequence of the higher electrolyte uptake by the in situ composite membrane. All the polymer electrolytes reported here exhibited ionic conductivity >4.5 mS cm^{-1} at 20 °C, which makes them suitable for the use in lithium batteries at room temperature.

The results of electrochemical stability tests of the polymer electrolytes by LSV are shown in Fig. 7. The polymer electrolyte based on P(VdF-HFP) without silica exhibits an anodic stability up to 4.5 V. With the incorporation of the electrochemically stable silica particles into the polymer matrix, the stability of the polymer electrolyte is further enhanced. Thus, for polymer electrolytes containing the in situ silica, the stability increases with the silica contents of 3, 6 and 9%, respectively, in the order: 4.5 < 4.6 < 4.7 V; while for the 6% directly added silica membrane the corresponding value is 4.6 V. The high anodic stability of these polymer electrolytes should render them potentially compatible with the high voltage cathode materials like $LiCoO_2$ and $LiMn_2O_4$ commonly used in lithium-ion batteries.

Fig. 8 presents the ac impedance data of the polymer electrolytes on lithium metal electrodes. The spectra is in the form of a semi-

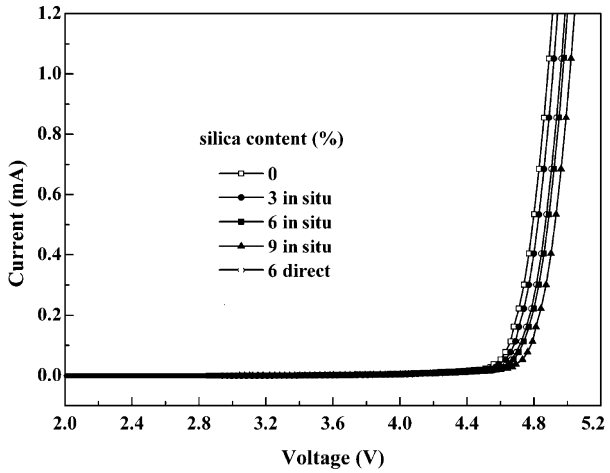

Fig. 7. Anodic stability by LSV of polymer electrolytes based on electrospun P(VdF-HFP) membranes with different silica contents (Li/polymer electrolyte/SS cells, 1 mV s^{-1}, 2–5.5 V).

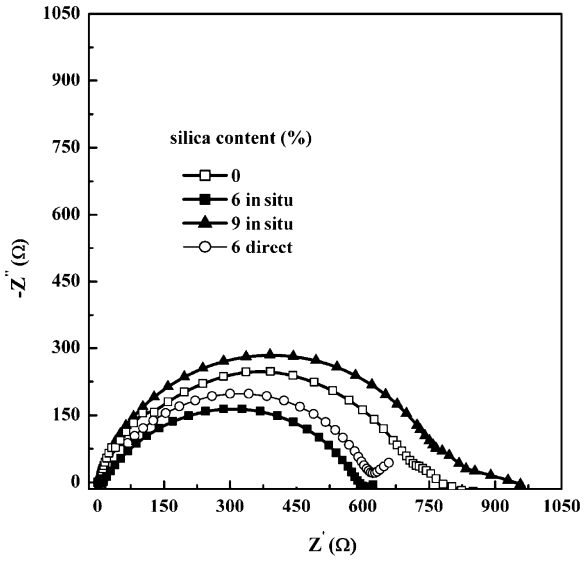

Fig. 8. ac impedance spectra of polymer electrolytes based on electrospun P(VdF-HFP) membranes with different silica contents (Li/ polymer electrolytes/Li cells, 10 mHz–2 MHz).

circle with the real axis intercept at high frequency end denoting bulk electrolyte resistance (R_b) and that at the low frequency end denoting the electrode/electrolyte interfacial resistance (R_f). The R_b values are low and lie in the range 4–10 Ω for the polymer electrolytes having an area of 2 cm^2, thus, denoting a sufficiently high ionic conductivity, as discussed earlier. R_f varies in the range of 600–900 Ω for the polymer electrolytes. The polymer electrolytes based on membranes with 6% silica have the lower values. At the higher silica content (9%) R_f is higher, and hence is not advantageous for forming a good interface on the lithium electrode.

The optimum polymer electrolytes with 6% of in situ and directly added silica have been evaluated for performance in Li/$LiFePO_4$ cells at room temperature. The first cycle charge–discharge properties at a current density corresponding to 0.1 C-rate are compared in Fig. 9. $LiFePO_4$ is a promising cathode-active material being considered for large scale battery applications in electric/hybrid vehicles, which has a discharge voltage of ~3.4 V and a theoretical specific capacity of 170 mAh g^{-1} [28]. The cell based on the polymer electrolyte with in situ silica delivers charge and discharge capacities of 170 mAh g^{-1}, which correspond to 100% utilization of the active

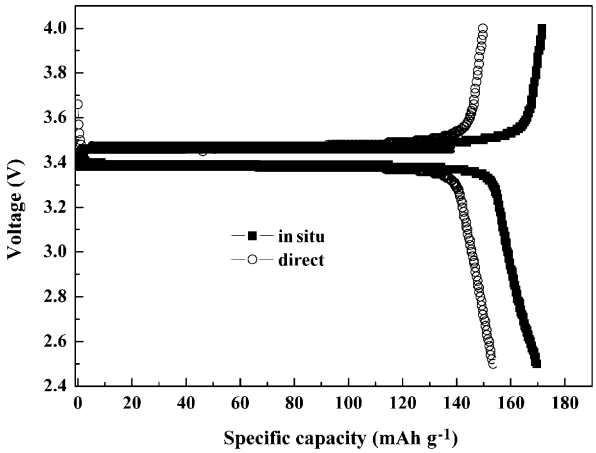

Fig. 9. Initial charge–discharge properties of Li/ polymer electrolyte/$LiFePO_4$ cells with polymer electrolytes based on electrospun P(VdF-HFP) membrane containing 6% of in situ generated silica and directly added silica (25 °C, 0.1 C-rate, 2.5–4.0 V).

material. The performance of the cell with polymer electrolyte containing directly added silica is lower, as a discharge capacity of 153 mAh g^{-1} was obtained. The enhanced performance of the polymer electrolyte with in situ generated silica is attributed mainly to its higher ionic conductivity and better compatibility with lithium metal. Further studies on the cycle performance and rate-capability of the cells with the promising polymer electrolyte containing 6% in situ silica are in progress.

4. Conclusions

Fibrous membranes have been prepared by electrospinning P(VdF-HFP) solutions containing in situ generated silica particles from 0 to 9 wt%. The novel composite membranes exhibit a porous morphology formed by interlaying of fibers of AFD ~1–2 μm. The polymer electrolytes prepared by activating the membranes with 1 M $LiPF_6$ in EC/DMC have been evaluated for electrochemical properties and suitability in lithium batteries. With a high porosity ~90%, the membranes exhibit electrolyte uptake of >550%. The optimum properties are exhibited by the polymer electrolyte based on the membrane with 6% in situ silica, which shows a maximum ionic conductivity of 8.06 mS cm^{-1} at 20 °C. The polymer electrolytes have anodic stability >4.5 V versus Li/Li^+ and show good compatibility with the lithium metal electrode. The suitability in Li/$LiFePO_4$ cell is demonstrated by exhibiting a 100% utilization of the cathode material at 0.1 C-rate at 25 °C. Incorporation of in situ generated silica has been observed to be more efficient in improving the properties than the directly added silica to the same extent in the polymer.

Acknowledgement

This research was supported by the Ministry of Knowledge Economy, Korea, under the Information Technology Research Center (ITRC) support program supervised by the Institute of Information Technology Assessment (IITA). G. Cheruvally and G.S. Chauhan gratefully acknowledge the Brain Pool Fellowship.

References

[1] M. Armand, J.M. Chabagno, M. Duclot, Fast Ion Transport in Solids, North-Holland, Amsterdam, 1979, p. 131.
[2] F. Capuano, F. Croce, B. Scrosati, J. Electrochem. Soc. 138 (1991) 1918.
[3] Z. Gadjourova, Y.G. Andreev, D.P. Tunstall, P.G. Bruce, Nature (London) 412 (2001) 520.
[4] C. Wang, T. Sakai, O. Watanabe, K. Hirahara, T. Nakanishi, J. Electrochem. Soc. 150 (2003) 1166.
[5] S.W. Choi, J.R. Kim, Y.R. Ahn, S.M. Jo, E.J. Cairns, Chem. Mater. 19 (2007) 104.
[6] X. Li, G. Cheruvally, J.K. Kim, J.W. Choi, J.H. Ahn, K.W. Kim, H.J. Ahn, J. Power Sources 167 (2007) 491.
[7] O. Bohnke, G. Frand, M. Rezrazzi, C. Rousselot, C. Truche, Solid State Ionics 66 (1993) 97.
[8] D. Peramunage, D.M. Pasquariello, K.M. Abraham, J. Electrochem. Soc. 42 (1995) 1789.
[9] D.E. Strauss, D. Golodnitsky, E. Peled, Electrochem. Solid State Lett. 2 (1999) 115.
[10] S.H. Chung, Y. Wang, L. Persi, F. Croce, S.G. Greenbaum, B. Scrosati, E. Plichta, J. Power Sources 97/98 (2001) 644.
[11] F. Croce, G.B. Appetecchi, L. Persi, B. Scrosati, Nature (London) 394 (1998) 456.
[12] G. Jiang, S. Maeda, H. Yang, Y. Saito, S. Tanase, T. Sakai, J. Power Sources 141 (2005) 143.
[13] Z. Wang, Z. Tang, Mater. Chem. Phys. 82 (2003) 16.
[14] J.M. Tarascon, A.S. Gozdz, C. Schmutz, F. Shokoohi, P.C. Warren, Solid State Ionics 86–88 (1996) 49.
[15] J.W. Choi, J.H. Kim, G. Cheruvally, J.H. Ahn, K.W. Kim, H.J. Ahn, J.U. Kim, J. Ind. Eng. Chem. 12 (2006) 939.
[16] A. Subramania, N.T. Kalyanasundaram, G. Vijayakumar, J. Power Sources 153 (2006) 177.
[17] J. Saunier, F. Alloin, J.Y. Sanchez, G. Caillon, J. Power Sources 119–121 (2003) 454.
[18] W. Pu, X. He, L. Wang, C. Jiang, C. Wan, J. Membr. Sci. 272 (2006) 11.

[19] J.W. Choi, J.K. Kim, G. Cheruvally, J.H. Ahn, H.J. Ahn, K.W. Kim, Electrochim. Acta 52 (2007) 2075.
[20] S.W. Choi, S.M. Jo, W.S. Lee, Y.R. Kim, Adv. Mater. 15 (2003) 2027.
[21] J.R. Kim, S.W. Choi, S.M. Jo, W.S. Lee, B.C. Kim, Electrochim. Acta 50 (2004) 69.
[22] S.S. Choi, Y.S. Lee, C.W. Joo, S.G. Lee, J.K. Park, K.S. Han, Electrochim. Acta 50 (2004) 339.
[23] S.W. Lee, S.W. Choi, S.M. Jo, B.D. Chin, D.Y. Kim, K.Y. Lee, J. Power Sources 163 (2006) 41.
[24] J.R. Kim, S.W. Choi, S.M. Jo, W.S. Lee, B.C. Kim, J. Electrochem. Soc. 152 (2005) A295.
[25] S.W. Choi, J.R. Kim, S.M. Jo, W.S. Lee, Y.R. Kim, J. Electrochem. Soc. 152 (2005) A989.
[26] X. He, Q. Shi, X. Zhou, C. Wan, C. Jiang, Electrochim. Acta 51 (2005) 1069.
[27] Y. Liu, J.Y. Lee, L. Hong, J. Power Sources 129 (2004) 303.
[28] J.K. Kim, J.W. Choi, G. Cheruvally, J.U. Kim, J.H. Ahn, G.B. Cho, K.W. Kim, H.J. Ahn, Mater. Lett. 61 (2007) 3822.
[29] Z.M. Huang, Y.Z. Zhang, M. Kotaki, S. Ramakrishna, Compos. Sci. Technol. 63 (2003) 2223.
[30] B. Soresi, E. Quartarone, P. Mustarelli, A. Magistris, G. Chiodelli, Solid State Ionics 166 (2004) 383.